

“GMA”-“GMAP” Inter-comparisons for the Full GMA Database Combined with the RAC Result for ${}^6\text{Li}(n,t)$

D.L. Smith*, V.G. Pronyaev

NDS, IAEA

* NDS Consultant

21 November 2003

The results shown in Fig. 1 to 13 were obtained from an inter-comparison of comparable runs using a common database and two distinct operating modes of the GMA code, “GMA” (original mode) and “GMAP” (a technical fix for the PPP effect is applied). Actually, one code, now designated as GMAP, can be operated in either of these two modes by the choice of a single control-switch parameter. The “GMAP” results presented here correspond to ordinary GMA-type runs coupled with the application of the technical solution to the PPP problem proposed by Chiba-Smith that was recently implemented in the code. The ENDF/B-VI evaluations (old standards) were adopted for use as non-informative priors in the runs that employed both the “GMA” mode and the “GMAP” mode. Since this prior is non-informative, some iteration is required for calculations in the “GMAP” mode. It was found that three iterations provided excellent convergence. The choice of the Chiba-Smith approach was based largely on the fact that it was very easy to implement in GMA (effectively just a single line of computational coding plus the addition of a control-switch option). This method gives results which, for the ${}^6\text{Li}(n,t)$ reaction test problem, agree reasonably well with the approaches suggested by Oh (Box-Cox) and Kawano (logarithmic transformation of the data). Since the agreement is quite good between the Chiba-Smith, Oh, and Kawano approaches, the former was used to produce GMAP because of the above-mentioned simplicity in coding this “fix”. Chen has suggested an alternative approach to dealing with PPP whereby the least-squares formalism remains unaltered but an algorithm is used to objectively down-weight highly discrepant data by modifying the original uncertainties. In fact, in the present analysis some modifications were also made to the database to enhance the errors of highly discrepant data. The detailed approach to handling the data is somewhat different to that of Chen but the underlying concept is similar.

The calculations that produced the attached figures were carried out as follows: A set of light-element data for ${}^6\text{Li}(n,t)$ that is essentially uncorrelated to the heavy element data was used separately in a RAC analysis by Chen. This analysis also incorporated certain data not included among the standards database but that correspond to other decay channels of the ${}^7\text{Li}$ compound nuclear system, thereby making use of the capability of the R-matrix formalism to fit such data simultaneously with the corresponding introduction of important physical constraints to the evaluated results for the standard reaction channel. Chen’s analysis produced a set of evaluated values for the ${}^6\text{Li}(n,t)$ reaction along with a covariance matrix. This information was introduced into code GMAP as a single data set along with all the remaining light-element data and heavy element data in the standards database in order to perform a combination by the least-squares method, both with and without the suggested “fix” for PPP. The partitioning of the experimental data used in the RAC R-matrix analysis from the remaining data sets that are essentially uncorrelated to the former avoided “double counting” of data sets by the combination procedure. By this means, the present exercise was designed to conform, as much as is possible at this time, to future runs that ultimately will generate the final intended standards evaluation.

A remaining task to be addressed by this work in the near future is the development of a procedure to introduce $^{10}\text{B}(n,\alpha_0)$ and $^{10}\text{B}(n,\alpha_1)$ cross-correlated information as one single data block in the GMA input. The full covariance/correlation matrix, which will include lower triangles for covariance matrices for $^{10}\text{B}(n,\alpha_0)$ and $^{10}\text{B}(n,\alpha_1)$ plus a rectangular block of cross-covariances/cross-correlations between these two reactions, should be provided by the R-matrix evaluators for use in the combining procedure with code GMAP.

The attached figures all show the difference obtained between the “GMAP” and “GMA” calculations for a common database along with the experimental data and their errors. By this means the degree to which the “GMAP” analysis “corrects” for PPP effects is demonstrated. The trend of the PPP effect, if not corrected, to produce results that are apparently “too low” is evident. In general, the magnitude of the PPP effect tends to become larger at the higher energies, most likely because the discrepancies there are also larger. In those reactions containing a very accurate thermal value included in the data set, the PPP effect is essentially non-existent at very low energies since the thermal value dominates the evaluation.

General conclusion is the following. Effects of PPP in GMA database are rather small, usually in the limits of 30% of uncertainty of the evaluated data. Small $^{235}\text{U}(n,f)$ cross section increase for E_n below 1 MeV will lead even to better agreement with the Godiva benchmark data.

The following specific comments apply to the indicated reactions:

$^6\text{Li}(n,t)$: small, up to 0.2% increase of the cross section is observed in the high energy of the “standard” region. Increase is in the limits of uncertainty of evaluated data.

$^6\text{Li}(n,n)$: no visible bias.

$^{10}\text{B}(n,\alpha_0)$: the presence of PPP is clearly seen for energy above 0.2 MeV.

$^{10}\text{B}(n,\alpha_1)$: the presence of PPP leads to an increase of the cross sections at the level of 30% of uncertainty of evaluated data for E_n below 0.2 MeV.

$^{10}\text{B}(n,n)$: small bias (0.3%) which is negligible compared with the uncertainty of the evaluated data.

$^{197}\text{Au}(n,\gamma)$: large PPP effect (1% bias) is observed.

$^{238}\text{U}(n,\gamma)$: large PPP effect (1 - 1.5% bias) is observed.

$^{235}\text{U}(n,f)$: local PPP effect is observed for E_n below 1 MeV and above 30 MeV. The bias above 30 MeV is 30% from uncertainty of the evaluated data.

$^{239}\text{Pu}(n,f)$: similar behaviour as for $^{235}\text{U}(n,f)$ with slightly larger bias.

$^{238}\text{U}(n,f)$: practically constant 0.2 – 0.3 % bias for E_n below 20 MeV and similar to the $^{235}\text{U}(n,f)$ and $^{239}\text{Pu}(n,f)$ behaviour for E_n above 30 MeV.

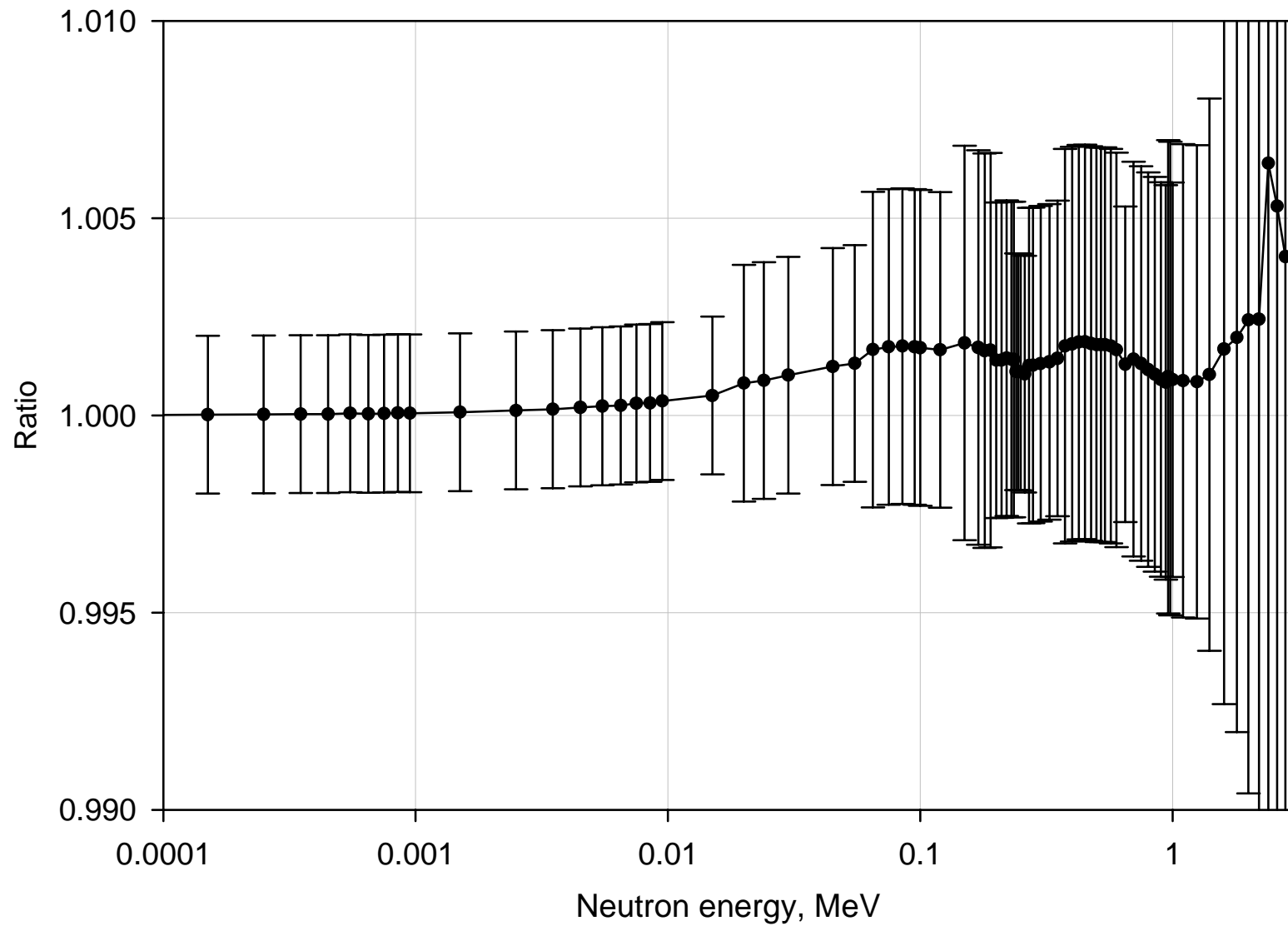


Fig. 1. Ratio of GMAP fit with using of Chiba-Smith option to exclude PPP to the standard GMA fit for ${}^6\text{Li}(n,t)$ reaction.

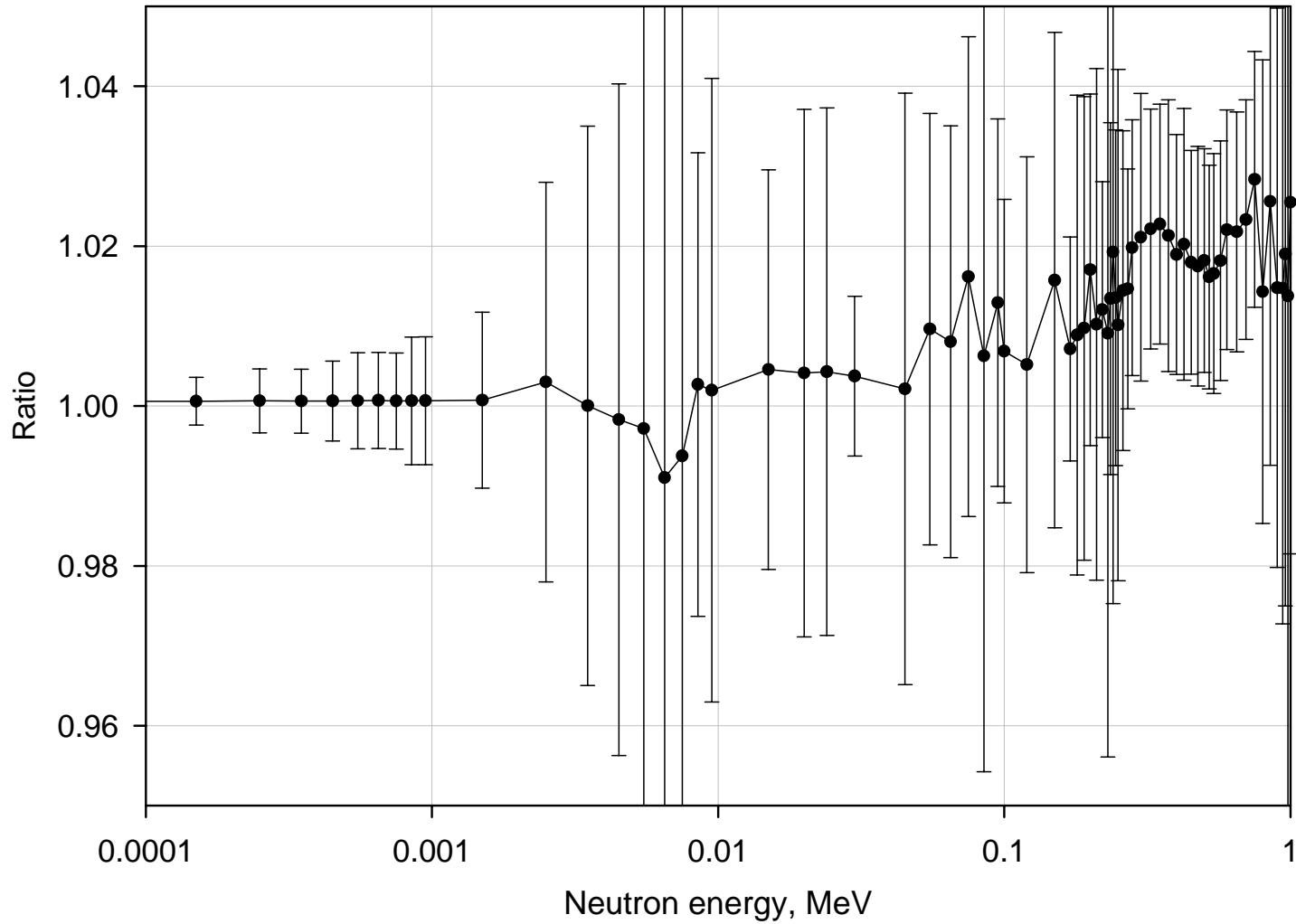


Fig. 3. Ratio of GMAP fit with using of Chiba-Smith option to exclude PPP to the standard GMA fit for $^{10}\text{B}(n, \alpha_0)$ reaction.

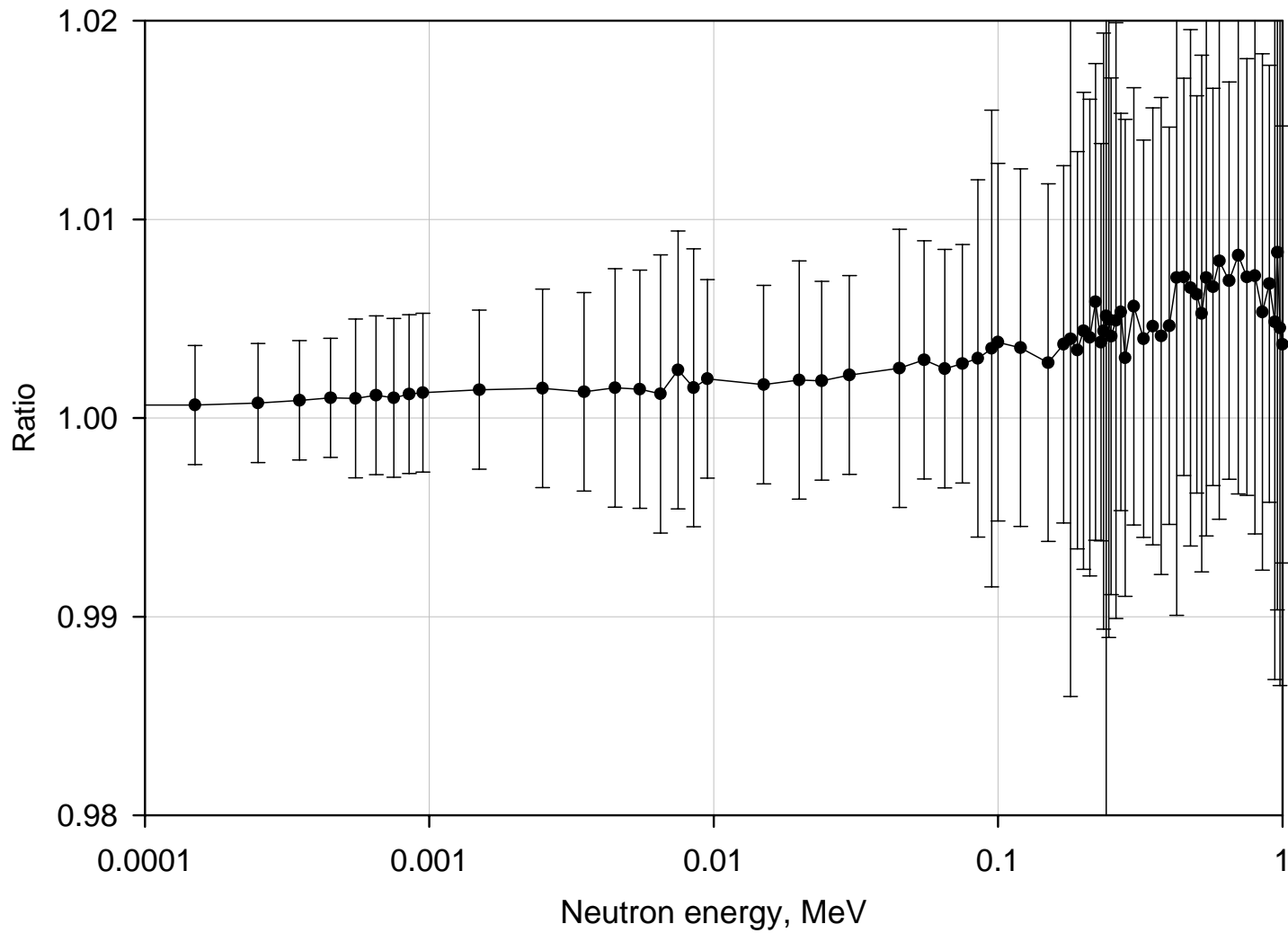


Fig. 4. Ratio of GMAP fit with using of Chiba-Smith option to exclude PPP to the standard GMA fit for $^{10}\text{B}(n,\alpha_1)$ reaction.

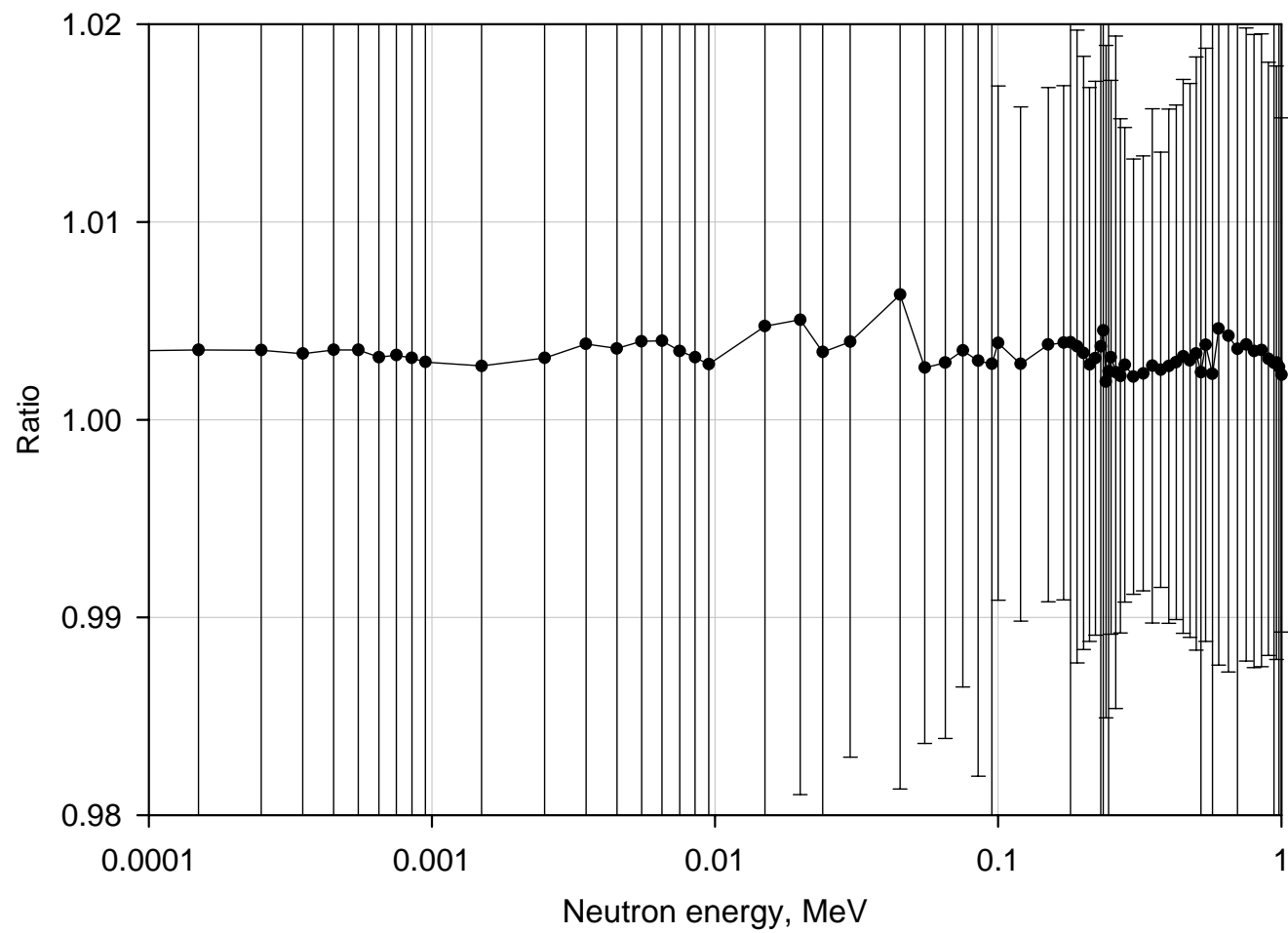


Fig. 5. Ratio of GMAP fit with using of Chiba-Smith option to exclude PPP to the standard GMA fit for $^{10}\text{B}(n,n)$ reaction.

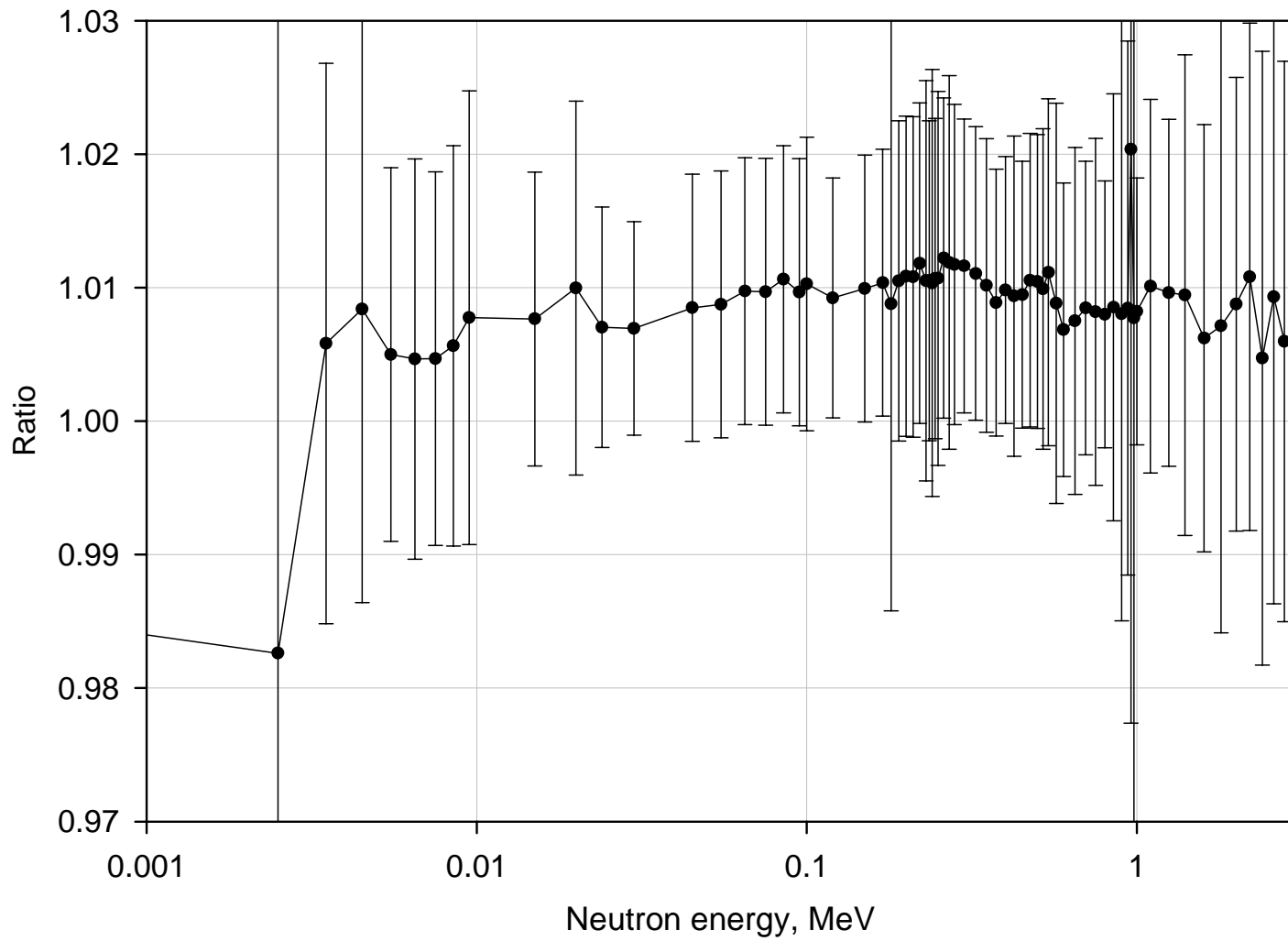


Fig. 6. Ratio of GMAP fit with using of Chiba-Smith option to exclude PPP to the standard GMA fit for $^{197}\text{Au}(n,\gamma)$ reaction.

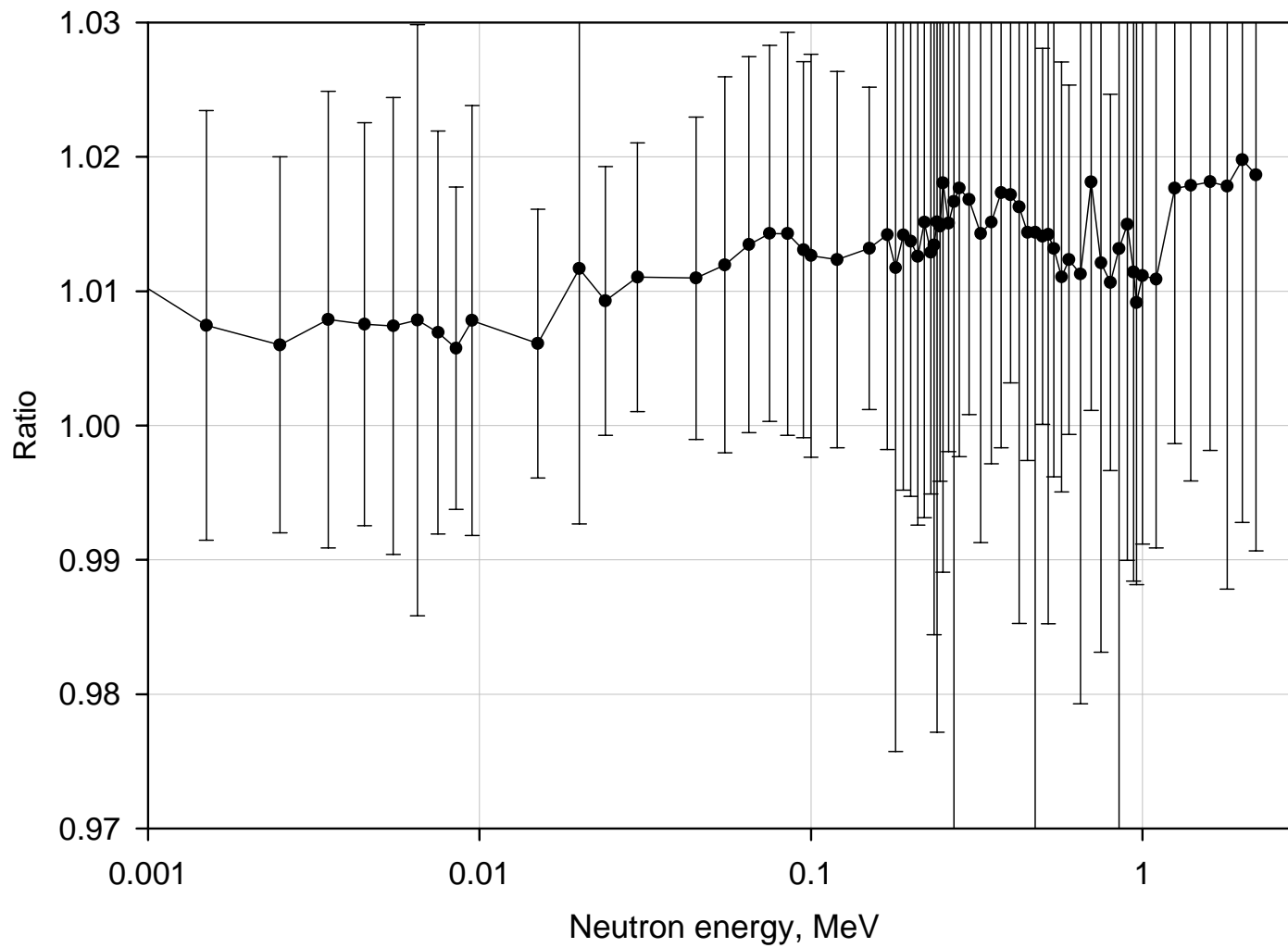


Fig. 7. Ratio of GMAP fit with using of Chiba-Smith option to exclude PPP to the standard GMA fit of $^{238}\text{U}(n,\gamma)$.

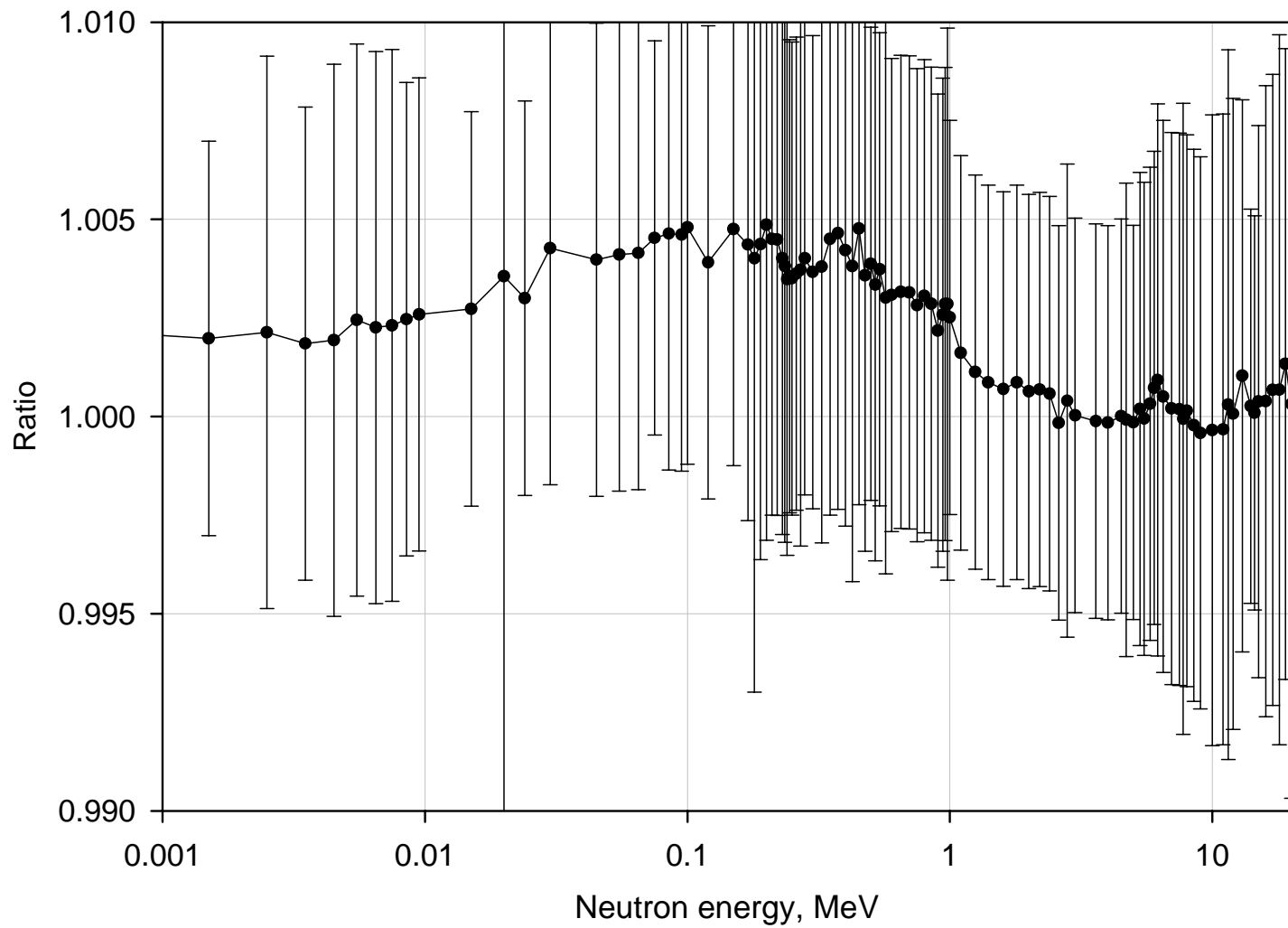


Fig. 8. Ratio of GMAP fit with using of Chiba-Smith option to exclude PPP to the standard GMA fit of $^{235}\text{U}(n,f)$.

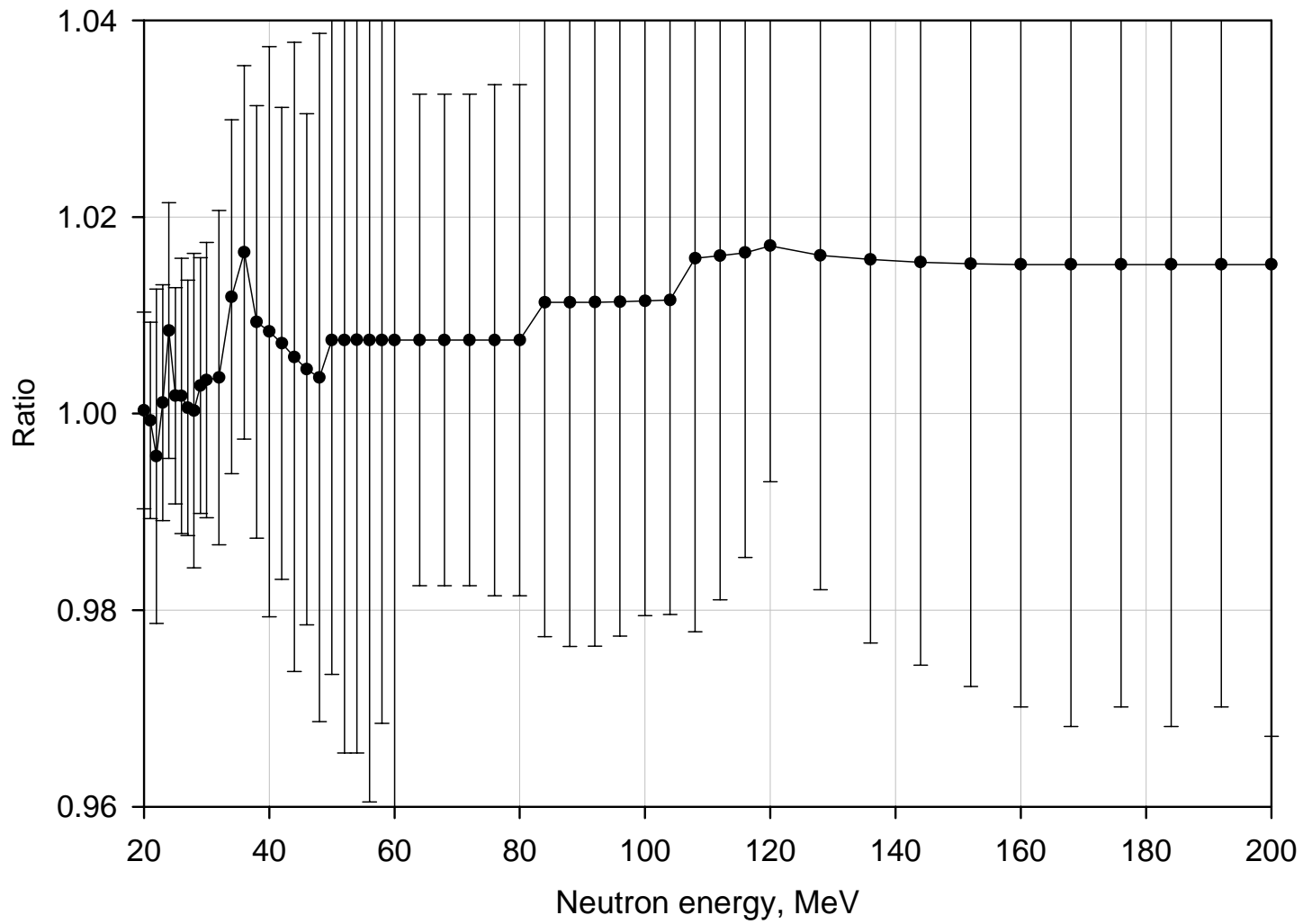


Fig. 9. Ratio of GMAP fit with using of Chiba-Smith option to exclude PPP to the standard GMA fit of $^{235}\text{U}(n,f)$.

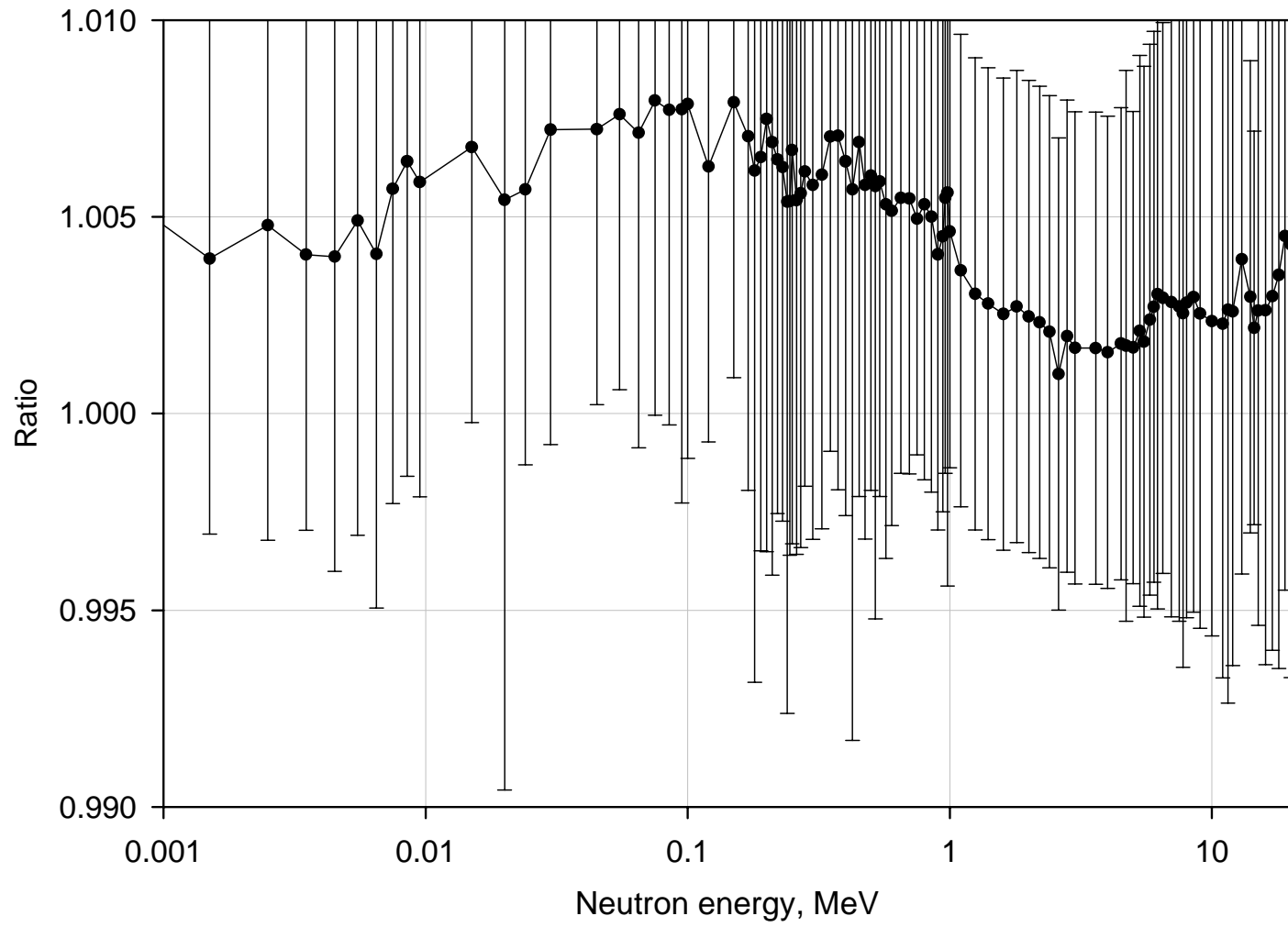


Fig. 10. Ratio of GMAP fit with using of Chiba-Smith option to exclude PPP to the standard GMA fit of $^{239}\text{Pu}(n,f)$.

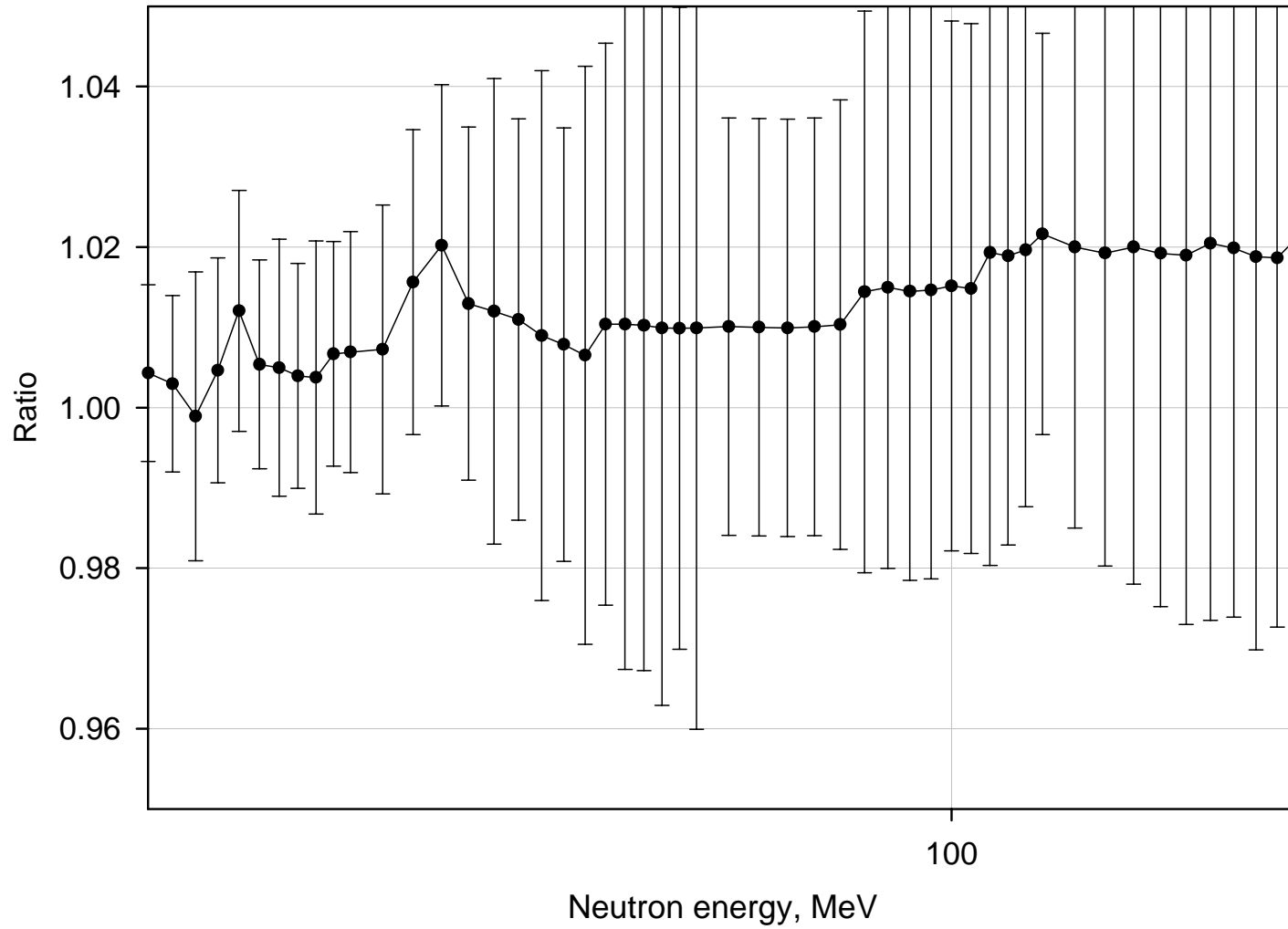


Fig. 11. Ratio of GMAP fit with using of Chiba-Smith option to exclude PPP to the standard GMA fit of $^{239}\text{Pu}(n,f)$.

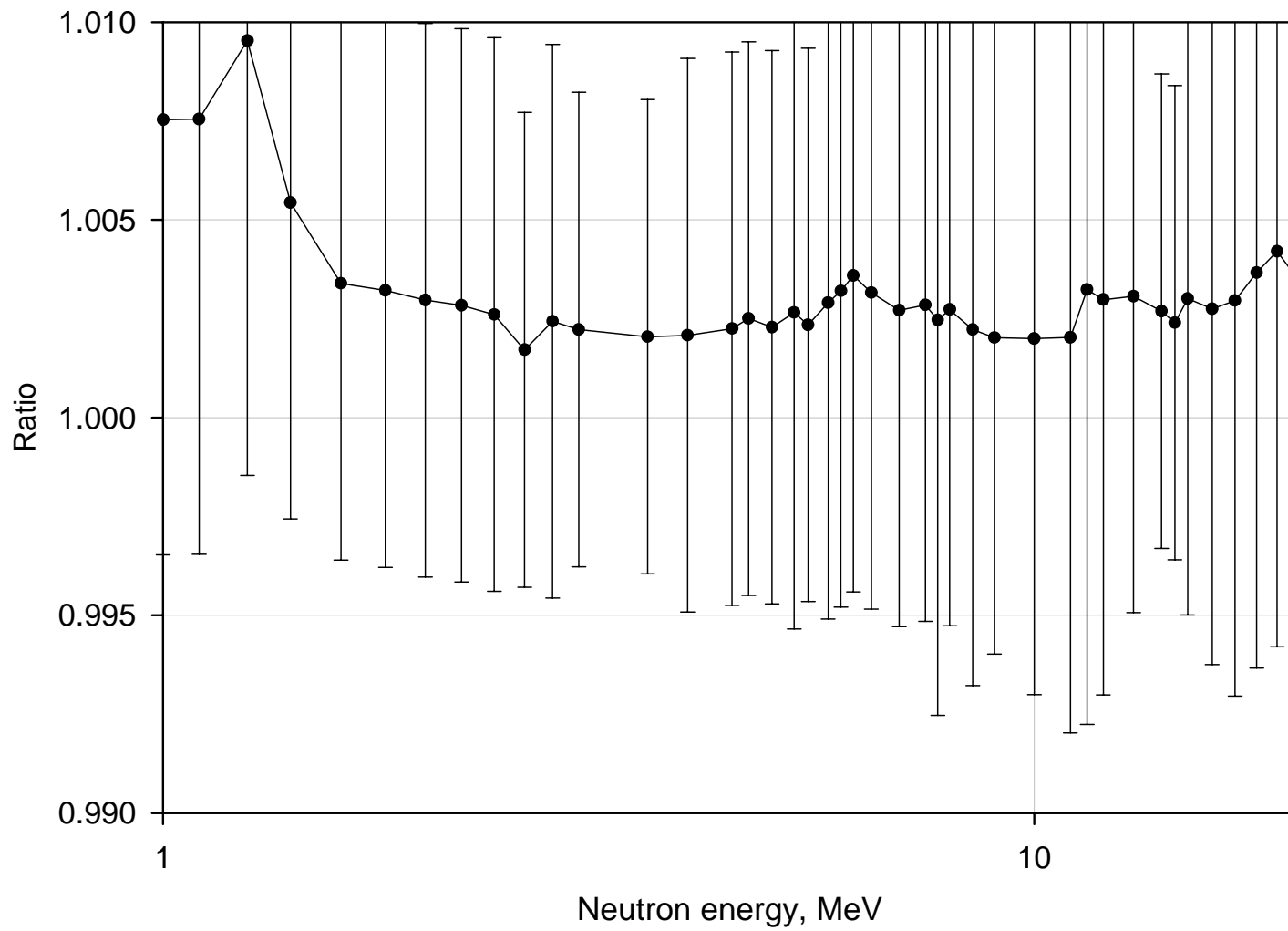


Fig. 12. Ratio of GMAP fit with using of Chiba-Smith option to exclude PPP to the standard GMA fit of $^{238}\text{U}(n,f)$.

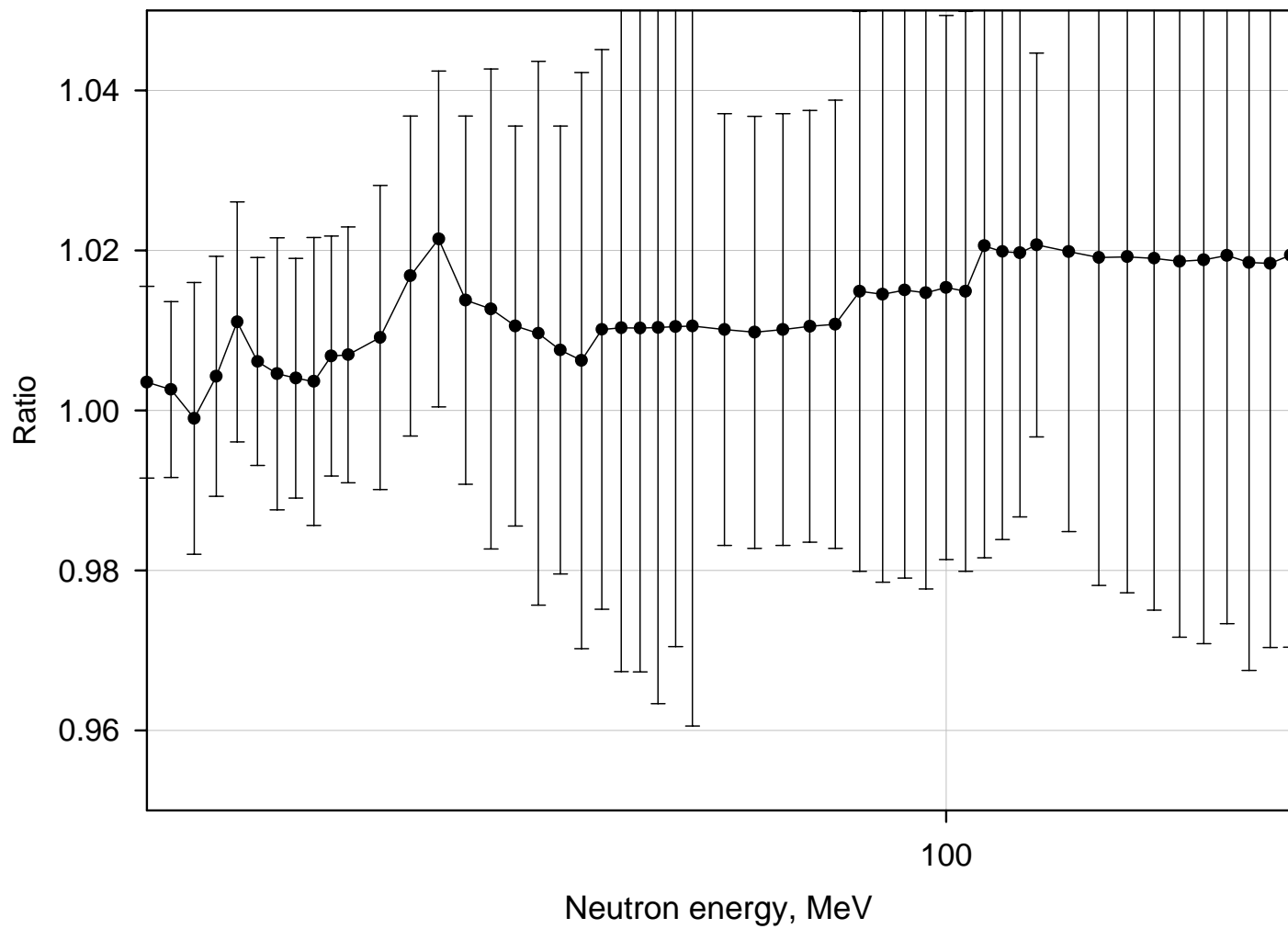


Fig. 13. Ratio of GMAP fit with using of Chiba-Smith option to exclude PPP to the standard GMA fit of $^{238}\text{U}(n,f)$.